This is an open access article published under a Creative Commons Attribution (CC-BY) License, which permits unrestricted use, distribution and reproduction in any medium, provided the author and source are cited.

ACS AUTHORCHOICE

OL | Organic Letters

pubs.acs.org/OrgLett

Letter

From Antiaromatic Norcorrolatonickel(II) to Aromatic and Nonaromatic Zwitterions: Innocent Ligands with Unbalanced Charge of the Core

Demin Ren, Oskar Smaga, Xinliang Fu, Xiaofang Li,* Miłosz Pawlicki, Sebastian Koniarz, and Piotr J. Chmielewski*

Cite This: *Org. Lett.* 2021, 23, 1032–1037

Read Online

ACCESS | Metrics & More | Article Recommendations | Supporting Information

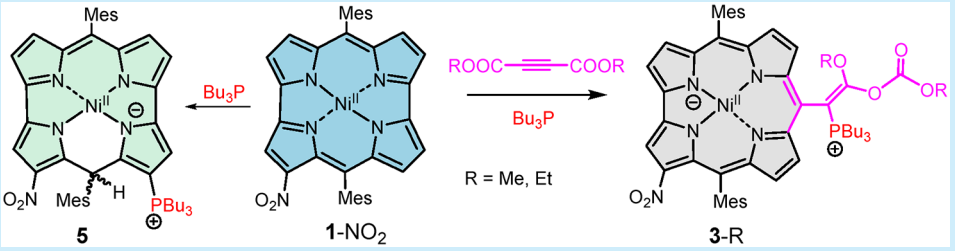

ABSTRACT: A three-component reaction of antiaromatic *meso*-mesityl-3-nitronorcorrolatonickel(II) **1**-NO_2 with dialkyl acetylenedicarboxylate and PBu_3 yields aromatic zwitterionic corrole nickel(II) complexes **3**-R with one of the *meso*-substituents comprising a positively charged tributyl phosphonium group and negatively charged coordination core. Reaction of **1**-NO_2 with PBu_3 alone resulted in a nonaromatic chiral adduct **5** of a zwitterionic phlorine character with a $-PBu_3^+$ group at a pyrrole β-position.

Norcorrrole is a tetrapyrrolic macrocycle of [16]-porphyrin(1.0.1.0) structure and antiaromatic character due to a 16π-electron delocalization pathway. The pioneering work of Bröring[1] followed by a gram-scale synthesis of norcorrole nickel(II) (Chart 1, **1**, R = mesityl) and copper(II)

Chart 1

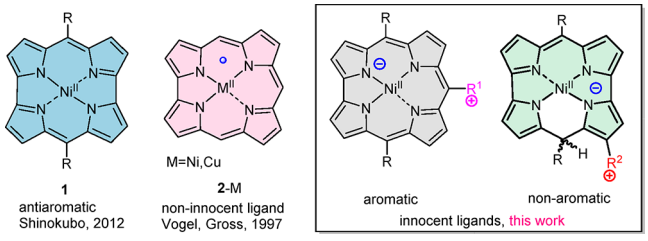

complexes introduced by Shinokubo et al.[2] opened an avenue for application of this porphyrinoid as an emblematic example of a stable and easy to handle antiaromatic system.[3] Complex **1** undergoes various substitution,[4] addition,[4e,g,5] or insertion[4g,5a,b,d] reactions. The inert metal ion in **1** secures planarity of the system adopting a square-planar geometry while dianionic ligand fully neutralizes electric charge of Ni^{2+}. This is unlike corrolatonickel(II) (Chart 1, **2**-Ni) where due to incompatibility of a tris(anionic) [18]porphyrin(1.1.1.0) ligand and divalent metal ion, the macrocycle acts as a noninnocent ligand of a π-radical electronic structure.[6] The radical form of the corrole ligand has been indicated in other corrole complexes,[6b,7] including those of zinc(II),[8] copper(II),[6a,9] or chloroiron(III).[10] Although some diamagnetic nickel(II) complexes of corrole derivatives or heteroanalogues, including *meso*-oxa-, -aza-, and -phosphacorroles have been reported,[5b,d,11] none of them consists of an unaltered aromatic corrole ring of an "all-carbon" perimeter.

In this paper, we report transformations of norcorrolatonickel(II) into diamagnetic corrolatonickel(II) or phlorine-like *meso*-hydronorcorrolatonickel(II) systems that are air-stable despite negatively charged coordination cores.

The three-component,[12] one-step, one-pot reaction of antiaromatic 3-nitro-5,14-dimesitylnorcorrolatonickel(II)[4f] (**1**-NO_2) with dimethyl or diethyl acetylenedicarboxylate (DMAD or DEAD) in the presence of tributylphosphine gave rise to the adducts **3**-Me or **3**-Et in about 50% yields (Scheme 1). The high-resolution ESI-MS(+) indicated addition of DMAD or DEAD and phosphine molecules (calcd 965.3791 $[M]^+$, obsd

Received: December 22, 2020
Published: January 21, 2021

See https://pubs.acs.org/sharingguidelines for options on how to legitimately share published articles.

ACS Publications

© 2021 The Authors. Published by American Chemical Society

https://dx.doi.org/10.1021/acs.orglett.0c04227
Org. Lett. 2021, 23, 1032–1037

Scheme 1. Reactions of 3-Nitronorcorrolatonickel(II) with Dialkyl Acetylenedicarboxylates and Tributylphosphine and Hydrolysis of the *Meso*-Substituent in the Adducts

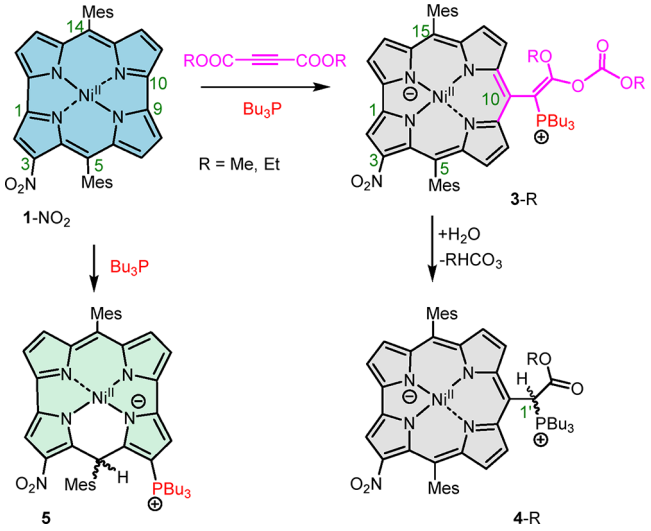

965.3800 for **3**-Me; calcd 993.4104 $[M]^+$, obsd 993.4101 for **3**-Et), while NMR confirmed the aromatic character of the formed corroles and the presence of a phosphonium group.

A plausible mechanism of the addition of the phosphine and DMAD or DEAD to **1**-NO_2 (Scheme S4 in SI) involves formation of an activated zwitterionic adduct composed of dialkyl acetylenedicarboxylate and Bu_3P.[12a] That intermediate adds regioselectively to the neighboring pyrrole α-carbons of the norcorrole (C9 and C10), thus forming a cyclopropane-containing transient species[12d] which then undergoes a series of rearrangements leading to **3**-R. The NMR indicated a C_1 symmetry of **3**-R. Their configurational stability allowed separation of enantiomers using a chiral stationary phase HPLC and recording of their weak CD spectra (Figure S55 in the SI). The structure of **3**-Et was confirmed by a single-crystal X-ray diffraction analysis (Figure 1A) revealing almost planar structure of the macrocycle and trigonal geometry of the ylide carbon C38 attached to the corrole *meso*-position.

The reaction of **1**-NO_2 with Bu_3P alone yielded a nonaromatic adduct **5** (Scheme 1) that was characterized by

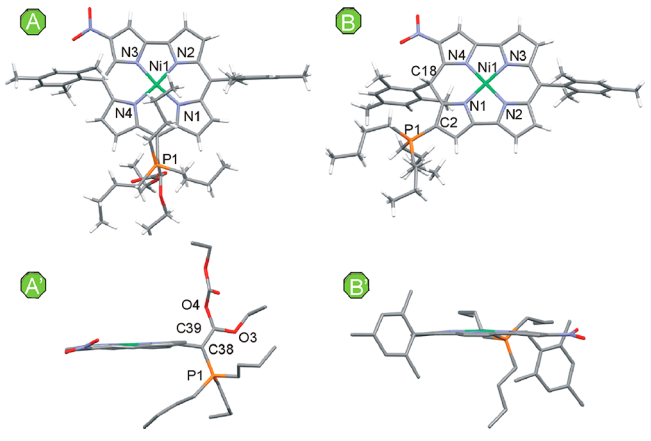

Figure 1. Stick diagrams of the molecular structures of **3**-Et (A and A′) and **5** (B and B′). In the side views A′ and B′ at the bottom, all hydrogens were removed, and in A′, both *meso*-mesityls were hidden for clarity.

ESI HRMS (calcd 822.3441 $[M - H]^+$, obsd 822.3389), multinuclear NMR, single crystal X-ray diffraction analysis (Figure 1B), UV−vis spectroscopy, and CD (Figure 2). Calculation of a Mulliken charge distribution in the DFT-optimized model of **5** indicated a positive charge on the phosphorus (+0.685) and, thus, trivalent phosphonium structure of the substituent and zwitterionic character of **5**, in line with the P1−C2 distance of 1.764(2) Å that is typical for a P−C(sp^2) single bond. A similar nonaromatic but not zwitterionic adduct has been very recently obtained in a reaction of **1** with N-heterocyclic carbene precursor.[5d] The zwitterionic character has been established for some bis-(corrole) free bases and antiaromatic deprotonated [28]-hexaphyrins(1.1.1.1.1.1).[13]

In both homologues **3**-R, the substituents attached to ylide carbon C38 are prone to hydrolysis (Scheme 1). The ESI(+) HRMS of the hydrolysis products indicated a loss of monoalkyl carbonate. ^{1}H NMR of the hydrolyzed species revealed the presence of two diastereomers **4**-R of equal populations due to a chiral center at the pyramidal carbon atom C1′ at the *meso*-position and the planar chirality of the whole system together giving rise to two pairs of enantiomers (Figure S57). They could not be effectively separated due to racemization which was completed within minutes at room temperature (Figures S57−S59 in the SI). The racemization was likely caused by a keto−enol tautomery occurring within the substituent, involving the proton transfer from the pyramidal carbon C1′ onto the carbonyl oxygen. The resulting tautomer **4′**-Et of trigonal C1′ was shown by the DFT calculations to be about 13.7 kcal/mol less stable than that with sp^3-hybridized C1′; thus, its population is expected to be undetectably low. Nevertheless, it may be a transient product upon the configuration change taking place at C1′ (Figure S59). Each diastereomer gave rise to a doublet of doublets at δ 6.62 or 6.66 ppm ($^2J_{PH}$ = 16.6 or 16.5 Hz and $^0J_{HH}$ = 0.8 or 0.7 Hz, respectively) due to 1′-H, correlating with a distinct ^{31}P nucleus resonating either at δ_P 35.7 or 35.5 ppm, respectively in a ^{1}H,^{31}P HMBC map. Interestingly, in a ^{1}H,^{1}H COSY, 1′-H correlated through-space with one of the adjacent β-pyrrole protons, i.e., either 8-H or 12-H (Figure S57C). Otherwise, the NMR characteristics of the stereoisomers **4**-R resemble those of the parent adducts **3**-R reflecting diamagnetic and aromatic character of the macrocycles. Chemical shifts calculated by the GIAO approach for the DFT-optimized structures of **3**-Et and **4**-Et satisfactorily match the experimental data (Figure S60). Also the electronic spectra of **3**-R and **4**-R are similar comprising a split Soret-type band in the region of 350−500 nm and an intense Q-type band near 615 nm with a shoulder tailing to 750 nm (Figure 2).

Spectrophotometric titrations of **3**-Et with trifluoroacetic acid (TFA) in DCM resulted in significant spectral changes (Figures S61 and S62) that could be only partially reversed by addition of a base. The ^{1}H NMR monitored titrations of zwitterions with TFA at low temperatures (Figures S63−S65 and S67−S74) revealed considerable broadening of all spectral lines of the starting substance that may indicate a paramagnetic character of the primary protonated species and its fast chemical exchange with the starting zwitterion (Scheme 2). Concurrently, at the temperatures below 253 K, a new set of sharp signals indicated formation of another protonation product $[H\text{-}3\text{-}R]^+$ (Scheme 2) with sp^3 hybridization of C17. Apart from the singlet of 2-H at δ 8.08 ppm, there were two AB systems typical for the pyrrole β-protons in the region of δ

https://dx.doi.org/10.1021/acs.orglett.0c04227
Org. Lett. 2021, 23, 1032−1037

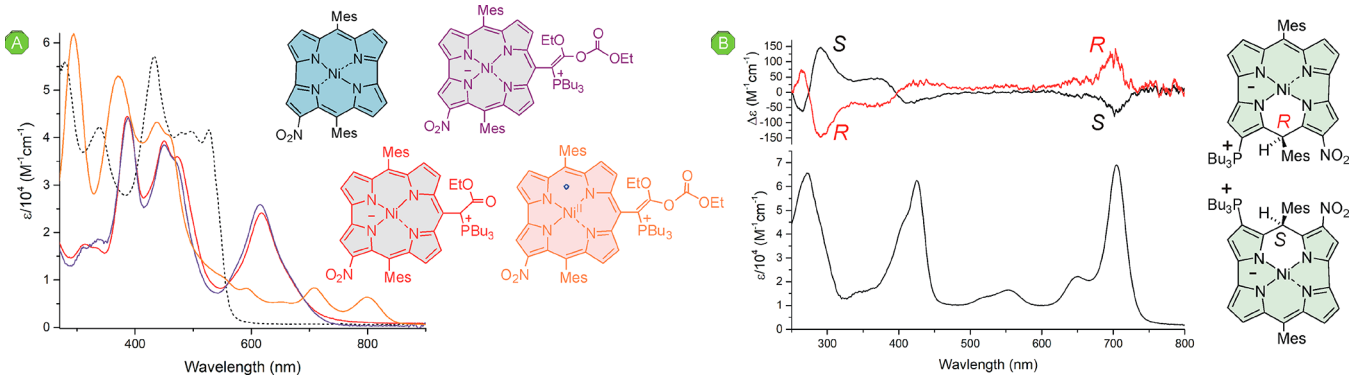

Figure 2. (A) Optical spectra (DCM, 298 K) of **3**-Et (purple), **4**-Et (red), and [**3**$^{\bullet}$-Et]I (orange). For comparison, the spectrum of **1**-NO_2 is included (dashed black trace). (B) Absorption (bottom) and CD (top) spectra (DCM, 298 K) of enantiomers of **5**.

Scheme 2. Protonation of 3-R

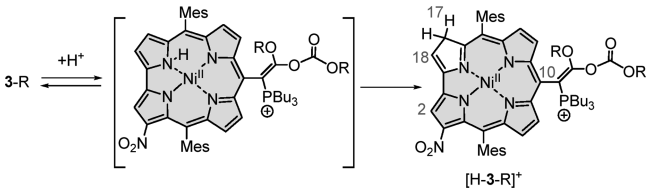

7.40−7.76 ppm and, quite unexpectedly, a triplet at δ 7.39 ppm (^3J = 2.8 Hz, **3**-Et, $CDCl_3$, 233 K) correlating in a COSY spectrum with two barely separated signals of diastereotopic protons of ABX system (^2J = 26.8 Hz, ^3J = 2.8 Hz) centered at δ 3.61 ppm (Figure 3). In the NOESY spectrum, the triplet signal correlate with the singlet of 2-H, thus allowing assignment the triplet to 18-H and the diastereotopic methylene to the site C17. Such a structure is apparently incompatible with a π-electron delocalization over the whole macrocyclic ring. Nevertheless, the system remains aromatic as it can be inferred from the values of the experimental and GIAO-calculated chemical shifts of protons, negative signs of NICS(1) calculated over the macrocycle as well as from the anisotropy of the induced current density (AICD)[14] revealing uninterrupted density delocalization in the macrocycle and clockwise orientation of the vectors (Figure 3). Analogous systems have been already reported more than a half century ago by Grigg et al.,[15] although aromaticity of those species has never been discussed.

The electrochemistry (Figures S79−S83, Table S3) showed reversible first and second oxidation processes (ox1, ox2) for all systems with potentials E_{ox1} ranging from −0.13 to 0.07 V and E_{ox2} at about 0.6 V (all potentials vs Fc/Fc^+ internal standard). The reductions occurring between −2.04 and −1.79 V were irreversible for **3**-R and **4**-R and reversible for **5**. Importantly, the first oxidation potentials E_{ox1} were by about 0.40−0.60 V lower than that of parent **1**-NO_2[4f] and from 0.5 to 1.5 V lower than observed for other metallocorroles.[6b] Remarkably, similarly low values of the oxidation potentials have been reported for the free base corrole monoanions ($[CorH_2]^-$) in pyridine or benzonitrile.[16]

Calculations of the charge distribution over the zwitterionic system **3**-Et with Multiwfn package[17] indicated delocalization of the net negative charge on the part of the macrocyclic ring (Figure 4). As expected, the positive charge resided mostly on the phosphonium moiety of the substituent at *meso*-carbon C10 (Figure 4B). The calculations performed for the models of

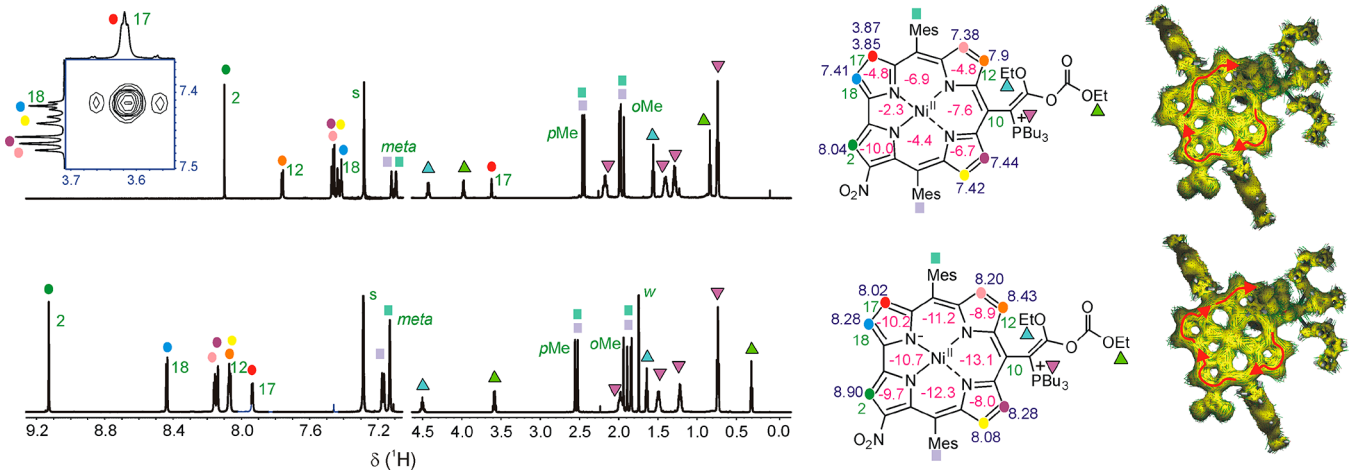

Figure 3. Comparison of the selected regions of ^{1}H NMR spectra (600 MHz, $CDCl_3$, 233 K) of **3**-Et (lower trace) and [H-**3**-Et]$^+$ (upper trace) along with partial peak assignments (green numbers and colored symbols: s, residual $CHCl_3$ signal; w, dissolved water signal), and AICD plots. The inset shows selected region of the COSY map of [H-**3**-Et]$^+$ presenting correlation of diastereotopic protons at C17 with the triplet of 18-H. The GIAO chemical shifts (ppm) of the pyrrole β-protons (purple numbers), and NICS(1) (rose numbers) at the central point of each of the rings are provided with the structures of the molecules.

https://dx.doi.org/10.1021/acs.orglett.0c04227
Org. Lett. 2021, 23, 1032−1037

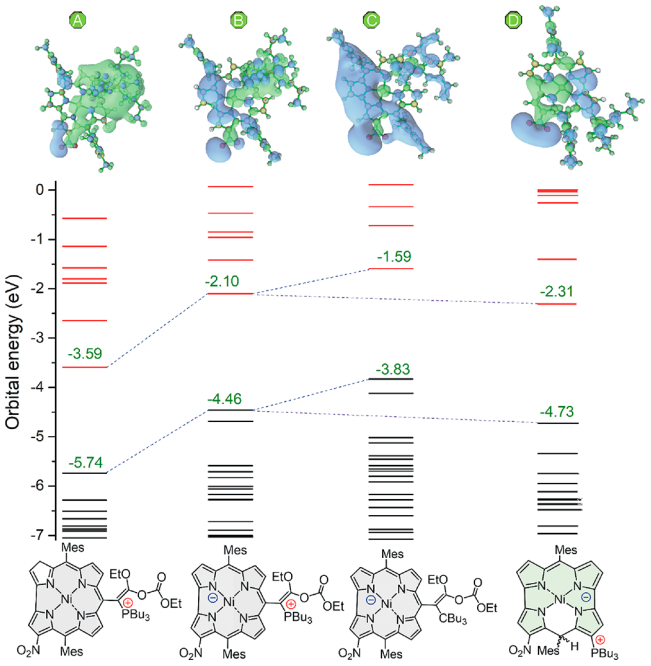

Figure 4. Comparison of charge distributions and the Kohn−Sham frontier orbital energies of [H-**3**-Et]$^+$ (A), **3**-Et (B), [**3**-Et-C]$^-$ (C), and **5** (D). The virtual orbital energy levels are colored in red. The negative and positive net charges are presented in blue and green, respectively, with an isosurface of 0.15 superimposed over the skeletons of the DFT-optimized structures.

one-electron oxidized ([**3**$^\bullet$-Et]$^+$) or protonated ([H-**3**-Et]$^+$) species showed no net negative charge on the macrocycle, unlike for a one-electron reduced corrole [**3**$^\bullet$-Et]$^-$ (Figure S84). In all these systems, the net positive charge is localized on the phosphonium group with a Mullikan charge on the P atom of about +0.75. To elucidate an effect of the cationic group on the charge distribution, we calculated DFT model of a virtual anionic system [**3**-Et-C]$^-$ where the phosphorus was exchanged by a carbon in the substituent at C10. The calculation indicated a considerable increase of the net negative charge on the macrocyclic ring (Figure 4C). As expected, the presence of the negative charge strongly destabilizes both filled and virtual orbitals (Figure 4). The HOMO energy in **3**-Et is by 1.28 eV higher than that in the cationic [H-**3**-Et]$^+$. On the other hand, the phosphonium moiety in **3**-Et stabilizes HOMO of the zwitterion by about 0.6 eV with respect to that of [**3**-Et-C]$^-$. The relation between the redox potentials of the first oxidation and the HOMO energy[18] accounted for the unique resilience of **3**-R and **4**-R to autoxidation. The oxidation potential estimated for [**3**-Et-C]$^-$ is about −0.7 V and for an analogue without $-NO_2$ substituent even below −0.9 V, which is close to the first reduction potential (−0.85 V) of the neutral corrolatonickel(II) radical formed upon oxidation of an elusive anionic complex with the atmospheric oxygen.[6]

Chemical oxidation of **3**-R or **4**-R solution in dichloromethane was carried out by addition of I_2 solution resulting in decrease of absorbance near 610 nm and formation of new bands at 709 and 800 nm in the UV−vis spectra (Figures 2, S85, S86, and S88A). Addition of iodine to the EPR-silent solutions of **3**-R or **4**-R gave rise to a featureless signal with g_0 = 2.0140 for the fluid solutions at room temperature (peak separation ∼8 G) and orthorhombic spectrum (g_1 = 2.0185, g_2 = 2.0074, g_3 = 2.0029, **3**-Et) for the frozen solution (77 K) indicating radical[6a,8] rather than nickel(III)[19] character of the cationic monooxidized species (Figures S87 and S88B). That conclusion was corroborated by the spin density calculation for [**3**$^\bullet$-Et]$^+$ indicating a negligible contribution of the metal orbitals to the SOMO (Figure S88C).

In summary, we have shown that antiaromatic norcorrole nickel(II) complex can be efficiently transformed into a diamagnetic and aromatic corrolatonickel(II) zwitterion that is stable toward autoxidation. The positively charged substituent as well as additional *meso*-carbon can be introduced by means of [2 + 1] cycloaddition of the in situ formed active phosphonium ylide and consecutive rearrangements taking place at the reaction site. These new corroles provide unique examples of stable neutral aromatic [18]porphyrin(1.1.1.0) systems with unbalanced negative charge of the macrocyclic core. The coordination, spectroscopic, and redox properties of these and analogous ligands with other metals will be further studied in our laboratories.

■ ASSOCIATED CONTENT

Supporting Information

The Supporting Information is available free of charge at https://pubs.acs.org/doi/10.1021/acs.orglett.0c04227.

Experimental and synthetic details, spectroscopic characterization, NMR, HRMS, UV−vis and CD spectra, electrochemical data, crystallographic data, and calculation details (PDF)

Accession Codes

CCDC 2040257−2040258 contain the supplementary crystallographic data for this paper. These data can be obtained free of charge via www.ccdc.cam.ac.uk/data_request/cif, or by emailing data_request@ccdc.cam.ac.uk, or by contacting The Cambridge Crystallographic Data Centre, 12 Union Road, Cambridge CB2 1EZ, UK; fax: +44 1223 336033.

■ AUTHOR INFORMATION

Corresponding Authors

Xiaofang Li − *Key Laboratory of Theoretical Organic Chemistry and Functional Molecules, Ministry of Education, School of Chemistry and Chemical Engineering, Hunan University of Science and Technology, Xiangtan, Hunan 411201, China*; Email: lixiaofang@hnust.edu.cn

Piotr J. Chmielewski − *Department of Chemistry, University of Wrocław, 50 383 Wrocław, Poland*; orcid.org/0000-0002-2548-6110; Email: piotr.chmielewski@chem.uni.wroc.pl

Authors

Demin Ren − *Key Laboratory of Theoretical Organic Chemistry and Functional Molecules, Ministry of Education, School of Chemistry and Chemical Engineering, Hunan University of Science and Technology, Xiangtan, Hunan 411201, China*

Oskar Smaga − *Department of Chemistry, University of Wrocław, 50 383 Wrocław, Poland*

Xinliang Fu − *Key Laboratory of Theoretical Organic Chemistry and Functional Molecules, Ministry of Education, School of Chemistry and Chemical Engineering, Hunan University of Science and Technology, Xiangtan, Hunan 411201, China*

https://dx.doi.org/10.1021/acs.orglett.0c04227
Org. Lett. 2021, 23, 1032−1037

Miłosz Pawlicki − *Department of Chemistry, University of Wrocław, 50 383 Wrocław, Poland; Department of Chemistry, Jagiellonian University, Gronostajowa 2 30 387, Kraków, Poland;* orcid.org/0000-0002-8249-0474
Sebastian Koniarz − *Department of Chemistry, University of Wrocław, 50 383 Wrocław, Poland*

Complete contact information is available at: https://pubs.acs.org/10.1021/acs.orglett.0c04227

Notes

The authors declare no competing financial interest.

■ ACKNOWLEDGMENTS

This work was supported by the National Natural Science Foundation of China (No. 21671063) and by the Polish National Science Center (2018/29/B/ST5/00280). M.P. thanks the Wrocław Supercomputer Centre (KDM WCSS) for sharing the computation space necessary for performing theoretical analysis.

■ DEDICATION

This paper is dedicated to Professor Lechosław Latos-Grażyński on the occasion of his 70th birthday.

■ REFERENCES

(1) Bröring, M.; Köhler, S.; Kleeberg, C. Norcorrole: Observation of the Smallest Porphyrin Variant with a N4 Core. *Angew. Chem., Int. Ed.* **2008**, *47*, 5658−5660.

(2) (a) Ito, T.; Hayashi, Y.; Shimizu, S.; Shin, J.-Y.; Kobayashi, N.; Shinokubo, H. Gram-Scale Synthesis of Nickel(II) Norcorrole: The Smallest Antiaromatic Porphyrinoid. *Angew. Chem., Int. Ed.* **2012**, *51*, 8542−8545. (b) Yonezawa, T.; Shafie, S. A.; Hiroto, S.; Shinokubo, H. Shaping Antiaromatic π-Systems by Metalation: Synthesis of a Bowl-Shaped Antiaromatic Palladium Norcorrole. *Angew. Chem., Int. Ed.* **2017**, *56*, 11822−11825.

(3) (a) Shin, J.-Y.; Yamada, T.; Yoshikawa, H.; Awaga, K.; Shinokubo, H. An Antiaromatic Electrode-Active Material Enabling High Capacity and Stable Performance of Rechargeable Batteries. *Angew. Chem., Int. Ed.* **2014**, *53*, 3096−3101. (b) Nozawa, R.; Tanaka, H.; Cha, W.; Hong, Y.; Hisaki, I.; Shimizu, S.; Shin, J.-Y.; Kowalczyk, T.; Irle, S.; Kim, D.; Shinokubo, H. Stacked antiaromatic porphyrins. *Nat. Commun.* **2016**, *7*, 13620. (c) Fujii, S.; Marqués-González, S.; Shin, J.-Y.; Shinokubo, H.; Masuda, T.; Nishino, T.; Arasu, N. P.; Vázquez, H.; Kiguchi, M. Highly-conducting molecular circuits based on antiaromaticity. *Nat. Commun.* **2017**, *8*, 15984. (d) Yamashina, M.; Tanaka, Y.; Lavendomme, R.; Ronson, T. K.; Pittelkow, M.; Nitschke, J. R. An antiaromatic-walled nanospace. *Nature* **2019**, *574*, 511−515. (e) Liu, S.-Y.; Kawashima, H.; Fukui, N.; Shinokubo, H. A 2-to-2′ 18-to-18′ doubly linked Ni(II) norcorrole dimer: An effectively conjugated antiaromatic dyad. *Chem. Commun.* **2020**, *56*, 6846−6849.

(4) (a) Nozawa, R.; Yamamoto, K.; Shin, J.-Y.; Hiroto, S.; Shinokubo, H. Regioselective Nucleophilic Functionalization of Antiaromatic Nickel(II) Norcorroles. *Angew. Chem., Int. Ed.* **2015**, *54*, 8454−8457. (b) Kawashima, H.; Hiroto, S.; Shinokubo, H. Acid-Mediated Migration of Bromide in an Antiaromatic Porphyrinoid: Preparation of Two Regioisomeric Ni(II) Bromonorcorroles. *J. Org. Chem.* **2017**, *82*, 10425−10432. (c) Yoshida, T.; Sakamaki, D.; Seki, S.; Shinokubo, H. Enhancing the low-energy absorption band and charge mobility of antiaromatic Ni^{II} norcorroles by their substituent effects. *Chem. Commun.* **2017**, *53*, 1112−1115. (d) Yoshida, T.; Shinokubo, H. Direct Amination of Antiaromatic NiII Norcorrole. *Mater. Chem. Front.* **2017**, *1*, 1853−1857. (e) Liu, B.; Li, X.; Stępień, M.; Chmielewski, P. J. Towards Norcorrin: Hydrogenation Chemistry and the Heterodimerization of Nickel(II) Norcorrole. *Chem. - Eur. J.* **2015**, *21*, 7790−7797. (f) Deng, Z.; Li, X.; Stępień, M.; Chmielewski, P. J. Nitration of Norcorrolatonickel(II): First Observation of a Diatropic Current in a System Comprising a Norcorrole Ring. *Chem. - Eur. J.* **2016**, *22*, 4231−4246. (g) Liu, B.; Yoshida, T.; Li, X.; Stępień, M.; Shinokubo, H.; Chmielewski, P. J. Reversible C-C Bond Breaking and Spin Equilibria in Bis(Pyrimidinenorcorrole). *Angew. Chem., Int. Ed.* **2016**, *55*, 13142−13146. (h) Li, X.; Meng, Y.; Yi, P.; Stępień, M.; Chmielewski, P. J. Pyridine-Fused Bis(Norcorrole) through Hantzsch-Type Cyclization: Enhancement of Antiaromaticity by an Aromatic Bridge. *Angew. Chem., Int. Ed.* **2017**, *56*, 10810−10814. (i) Ren, D.; Fu, X.; Li, X.; Koniarz, S.; Chmielewski, P. J. Reaction of antiaromatic porphyrinoid with active methylene compounds. *Org. Chem. Front.* **2019**, *6*, 2924−2933.

(5) (a) Fukuoka, T.; Uchida, K.; Sung, Y. M.; Shin, J.-Y.; Ishida, S.; Lim, J. M.; Hiroto, S.; Furukawa, K.; Kim, D.; Iwamoto, T.; Shinokubo, H. Near-IR Absorbing Nickel(II) Porphyrinoids Prepared by Regioselective Insertion of Silylenes into Antiaromatic Nickel(II) Norcorrole. *Angew. Chem., Int. Ed.* **2014**, *53*, 1506−1509. (b) Liu, S.-Y.; Tanaka, H.; Nozawa, R.; Fukui, N.; Shinokubo, H. Synthesis of *meso*-Alkyl-Substituted Norcorrole Ni^{II} Complexes and Conversion to 5-Oxaporphyrins(2.0.1.0). *Chem. - Eur. J.* **2019**, *25*, 7618−7622. (c) Fu, X.; Meng, Y.; Li, X.; Stępień, M.; Chmielewski, P. J. Extension of antiaromatic norcorrole by cycloaddition. *Chem. Commun.* **2018**, *54*, 2510−2513. (d) Liu, S.-Y.; Fukuoka, T.; Fukui, N.; Shin, J.-Y.; Shinokubo, H. Reactions of Antiaromatic Norcorrole Ni(II) Complex with Carbenes. *Org. Lett.* **2020**, *22*, 4400−4403.

(6) (a) Will, S.; Lex, J.; Vogel, E.; Schmickler, H.; Gisselbrecht, J.-P.; Haubtmann, C.; Bernard, M.; Gross, M. Nickel and Copper Corroles: Well-Known Complexes in a New Light. *Angew. Chem., Int. Ed. Engl.* **1997**, *63*, 357−361. (b) Ghosh, A. Electronic Structure of Corrole Derivatives: Insights from Molecular Structures, Spectroscopy, Electrochemistry, and Quantum Chemical Calculations. *Chem. Rev.* **2017**, *117*, 3798−3881. (c) Ghosh, A.; Wondimagegn, T.; Parusel, A. B. J. Electronic Structure of Gallium, Copper, and Nickel Complexes of Corrole. High-Valent Transition Metal Centers versus Non-innocent Ligands. *J. Am. Chem. Soc.* **2000**, *122*, 5100.

(7) Ghosh, A.; Steene, E. High-valent transition metal centers versus noninnocent ligands in metallocorroles: insights from electrochemistry and implications for high-valent heme protein intermediates. *J. Inorg. Biochem.* **2002**, *91*, 423−436.

(8) Schweyen, P.; Brandhorst, K.; Wicht, R.; Wolfram, B.; Bröring, M. The Corrole Radical. *Angew. Chem., Int. Ed.* **2015**, *54*, 8213−8216.

(9) Bröring, M.; Brégier, F.; Tejero, E. C.; Hell, Ch.; Holthausen, M. C. Revisiting the Electronic Ground State of Copper Corroles. *Angew. Chem., Int. Ed.* **2007**, *46*, 445−448.

(10) (a) Krzystek, J.; Schnegg, A.; Aliabadi, A.; Holldack, K.; Stoian, A.; Ozarowski, A.; Hicks, S. D.; Abu-Omar, M. M.; Thomas, K. E.; Ghosh, A.; Caulfield, K. P.; Tonzetich, Z. J.; Telser, J. Advanced Paramagnetic Resonance Studies on Manganese and Iron Corroles with a Formal d^4 Electron Count. *Inorg. Chem.* **2020**, *59*, 1075−1090. (b) Cai, S.; Walker, F. A.; Licoccia, S. NMR and EPR Investigations of Iron Corrolates: Iron(III) Corrolate Cation Radicals or Iron(IV) Corrolates? *Inorg. Chem.* **2000**, *39*, 3466−3478. (c) Zakharieva, O.; Schunemann, V.; Gerdan, M.; Licoccia, S.; Walker, F. A.; Trautwein, A. X. Is the Corrolate Macrocycle Innocent or Noninnocent? Magnetic Susceptibility, Mössbauer, ^1H NMR, and DFT Investigations of Chloro- and Phenyliron Corrolates. *J. Am. Chem. Soc.* **2002**, *124*, 6636−6648. (d) Cai, S.; Licoccia, S.; D'Ottavi, C.; Paolesse, R.; Nardis, S.; Bulach, V.; Zimmer, B.; Shokhireva, T. K.; Walker, F. A. Chloroiron meso-triphenylcorrolates: electronic ground state and spin delocalization. *Inorg. Chim. Acta* **2002**, *339*, 171−178. (e) Stefanelli, M.; Nardis, S.; Tortora, L.; Fronczek, F. R.; Smith, K. M.; Licoccia, S.; Paolesse, R. Nitration of iron corrolates: further evidence for non-innocence of the corrole ligand. *Chem. Commun.* **2011**, *47*, 4255−4257. (f) Ye, S.; Tuttle, T.; Bill, E.; Simkhovich, L.; Gross, Z.; Thiel, W.; Neese, F. The Electronic Structure of Iron Corroles: A Combined Experimental and Quantum Chemical Study. *Chem. - Eur. J.* **2008**, *14*, 10839−10851.

(11) (a) Ruppert, R.; Jeandon, C.; Callot, H. J. Nonaromatic Corroles: Regioselectivity of Electrophilic Substitution. *J. Org. Chem.* **2008**, *73*, 694−700. (b) Horie, M.; Hayashi, Y.; Yamaguchi, S.;

Shinokubo, H. Synthesis of Nickel(II) Azacorroles by Pd-Catalyzed Amination of α,α′-Dichlorodipyrrin Ni^{II} Complex and Their Properties. *Chem. - Eur. J.* **2012**, *18*, 5919−5923. (c) Omori, H.; Shinokubo, H. Ni(II) 10-Boracorrole: An Antiaromatic Porphyrinoid Containing a Boron Atom at the meso-Position. *Organometallics* **2019**, *38*, 2878−2882. (d) Jeandon, C.; Ruppert, R.; Callot, H. J. Acylation of Nickel meso-Tetraarylporphyrins: Porphyrin to Corrole Ring Contraction and Formation of seco-Porphyrins. *J. Org. Chem.* **2006**, *71*, 3111−3120. (e) Omori, H.; Hiroto, S.; Takeda, Y.; Fliegl, H.; Minakata, S.; Shinokubo, H. Ni(II) 10-Phosphacorrole: A Porphyrin Analogue Containing Phosphorus at the Meso Position. *J. Am. Chem. Soc.* **2019**, *141*, 4800−4805.

(12) (a) Ramazani, A.; Kazemizadeh, A. R.; Ahmadi, E.; Noshiranzadeh, N.; Souldozi, A. Synthesis and Reactions of Stabilized Phosphorus Ylides. *Curr. Org. Chem.* **2008**, *12*, 59−82. (b) Gupta, S.; Aggarwal, K.; Khurana, J. M. Synthesis of Novel Functionalized Triphenylphosphanylidene-Spirobarbiturates through a Three-Component Reaction. *ChemistrySelect* **2018**, *3*, 4110−4113. (c) Aitken, R. A.; Costello, S. J.; Slawin, A. M. Z.; Wilson, N. J. A New Crystalline Zwitterionic Product from the Reaction of Bu3P and DMAD. *Eur. J. Org. Chem.* **2003**, *2003*, 623−625. (d) Chuang, S.-C.; Santhosh, K. C.; Lin, C.-H.; Wang, S.-L.; Cheng, C.-H. Synthesis and Chemistry of Fullerene Derivatives Bearing Phosphorus Substituents. Unusual Reaction of Phosphines with Electron-Deficient Acetylenes and C_{60}. *J. Org. Chem.* **1999**, *64*, 6664−6669.

(13) (a) Hiroto, S.; Aratani, N.; Shibata, N.; Higuchi, Y.; Sasamori, T.; Tokitoh, N.; Shinokubo, H.; Osuka, A. Zwitterionic Corroles: Regioselective Nucleophilic Pyridination of a Doubly Linked Biscorrole. *Angew. Chem., Int. Ed.* **2009**, *48*, 2388−2390. (b) Naoda, K.; Osuka, A. A Doubly Zwitterionic Antiaromatic [28]Hexaphyrin Formed upon Deprotonation of 5,20-Di(N-methyl-4-pyridinium)-Substituted [28]Hexaphyrin. *Chem. - Asian J.* **2016**, *11*, 2849−2853.

(14) Geuenich, D.; Hess, K.; Köhler, F.; Herges, R. Anisotropy of the Induced Current Density (ACID), a General Method To Quantify and Visualize Electronic Delocalization. *Chem. Rev.* **2005**, *105*, 3758−3772.

(15) (a) Grigg, R.; Johnson, A. W.; Shelton, K. W. Alkylations and Thermal Sigmatropic Rearrangements of Nickel 1-Methyltetradehydrocorrins. *J. Chem. Soc. C* **1968**, 1291−1296. (b) Grigg, R.; Johnson, A. W.; Richardson, K.; Smith, M. J. Thermal Rearrangement of Nickel 1-Substituted Tetradehydrocorrins. *J. Chem. Soc. C* **1970**, 1289−1295. (c) Grigg, R.; Johnson, A. W.; Shelton, G. The Structures and Thermal Rearrangements of Alkylated Palladium and Copper Corroles. *J. Chem. Soc. C* **1971**, 2287−2294.

(16) Shen, J.; Shao, J.; Ou, Z.; E, W.; Koszarna, B.; Gryko, D. T.; Kadish, K. M. Electrochemistry and Spectroelectrochemistry of meso-Substituted Free-Base Corroles in Nonaqueous Media: Reactions of $(Cor)H_3$, $[(Cor)H_4]^+$, and $[(Cor)H_2]^-$. *Inorg. Chem.* **2006**, *45*, 2251−2265.

(17) Lu, T.; Chen, F. Multiwfn: A Multifunctional Wavefunction Analyzer. *J. Comput. Chem.* **2012**, *33*, 580−592.

(18) (a) Trasatti, S. The Absolute Electrode Potential: An Explanatory Note (Recommendations 1986). *J. Electroanal. Chem. Interfacial Electrochem.* **1986**, *209*, 417−428. (b) Czichy, M.; Zhylitskaya, H.; Zassowski, P.; Navakouski, M.; Chulkin, P.; Janasik, P.; Lapkowski, M.; Stępień, M. Electrochemical Polymerization of Pyrrole−Perimidine Hybrids: Low-Bandgap Materials with High n-Doping Activity. *J. Phys. Chem. C* **2020**, *124*, 14350−14362. (c) Méndez-Hernández, D. D.; Tarakeshwar, P.; Gust, D.; Moore, T. A.; Moore, A. L.; Mujica, V. Simple and accurate correlation of experimental redox potentials and DFT-calculated HOMO/LUMO energies of polycyclic aromatic hydrocarbons. *J. Mol. Model.* **2013**, *19*, 2845−2848.

(19) (a) Chmielewski, P. J.; Latos-Grażyński, L. EPR and ^2H NMR Studies on the Oxidation of Nickel(II) 2-Aza-21-Carbatetraphenylporphyrin to Form Novel Organometallic Nickel(III) Complexes. *Inorg. Chem.* **1997**, *36*, 840−845. (b) Schmidt, I.; Chmielewski, P. J.; Ciunik, Z. Alkylation of the Inverted Porphyrin Nickel(II) Complex by Dihalogenalkanes: Formation of Monomeric and Dimeric Derivatives. *J. Org. Chem.* **2002**, *67*, 8917−8927. (c) Schmidt, I.; Chmielewski, P. J. Nickel(II) Complexes of 21-C-Alkylated Inverted Porphyrins: Synthesis, Protonation, and Redox Properties. *Inorg. Chem.* **2003**, *42*, 5579−5593. (d) Chmielewski, P. J. Synthesis, Structure, and Redox Properties of N-Confused Bis-(porphyrinatonickel(II)) Linked by o-Xylene. *Inorg. Chem.* **2007**, *46*, 1617−1626.

https://dx.doi.org/10.1021/acs.orglett.0c04227
Org. Lett. 2021, 23, 1032−1037